

# RSC Advances



This is an *Accepted Manuscript*, which has been through the Royal Society of Chemistry peer review process and has been accepted for publication.

*Accepted Manuscripts* are published online shortly after acceptance, before technical editing, formatting and proof reading. Using this free service, authors can make their results available to the community, in citable form, before we publish the edited article. This *Accepted Manuscript* will be replaced by the edited, formatted and paginated article as soon as this is available.

You can find more information about *Accepted Manuscripts* in the [Information for Authors](#).

Please note that technical editing may introduce minor changes to the text and/or graphics, which may alter content. The journal's standard [Terms & Conditions](#) and the [Ethical guidelines](#) still apply. In no event shall the Royal Society of Chemistry be held responsible for any errors or omissions in this *Accepted Manuscript* or any consequences arising from the use of any information it contains.

1 **Ammonia removal from water using sodium hydroxide modified**  
2 **zeolite mordenite**

3  
4 Jennifer Pieter Soetardji<sup>1,§</sup>, Jeannete Cindy Claudia<sup>1,§</sup>, Yi-Hsu Ju<sup>2</sup>, Joseph A Hriljac<sup>3</sup>, Tzu-Yu  
5 Chen<sup>3</sup>, Felycia Edi Soetaredjo<sup>1,\*</sup>, Shella Permatasari Santoso<sup>2</sup>, Alfin Kurniawan<sup>2</sup>, Suryadi  
6 Ismadji<sup>1,\*</sup>

7  
8 <sup>1</sup> Department of Chemical Engineering, Widya Mandala Surabaya Catholic University,  
9 Kalijudan 37, Surabaya 60114, Indonesia

10 <sup>2</sup> Department of Chemical Engineering, National Taiwan University of Science and  
11 Technology, No. 43, Sec. 4, Keelung Rd., Taipei City 106, Taiwan (R.O.C)

12 <sup>3</sup> School of Chemistry, University of Birmingham, Edgbaston, Birmingham B15 2TT UK

13  
14 § These authors contribute equally.

15 \* Corresponding authors: e-mail address: felyciae@yahoo.com, Tel.: +62 31 389 1264, Fax:  
16 +62 31 389 1267; suryadiismadji@yahoo.com

17

18

19

**Abstract**

20 Natural and modified mordenite zeolites were used to remove ammonium ions from aqueous  
21 solution and Koi pond water. The zeolite modification was conducted using sodium  
22 hydroxide solutions of different strengths at 75°C for 24 h. Langmuir, Freundlich, Sips, and  
23 Toth equations with their temperature dependent forms were used to represent the adsorption  
24 equilibria data. The Langmuir and its temperature dependent forms could represent the data  
25 better than the other models. The pseudo-first order has better performance than pseudo-  
26 second order in correlating the adsorption kinetic data. The controlling mechanism of the  
27 adsorption of  $\text{NH}_4^+$  from aqueous solution onto the natural zeolite and the one treated with  
28 6M sodium hydroxide solution was dominated by physical adsorption. The competition with  
29 other ions occurred through different reaction mechanisms so it decreases the removal  
30 efficiency of ammonium ions by the zeolites. For the treated zeolite, the removal efficiency  
31 decreased from 81% to 66.9%. A Thomas model can represent the experimental data for both  
32 adsorption of ammonia from aqueous solution or from Koi pond water.

33

34

35

36

37

38 **Keywords:** Zeolite; Mordenite, Sodium hydroxide; Ammonium removal; Adsorption  
39 isotherm; Kinetic; Breakthrough

## 40 INTRODUCTION

41 The presence of ammonia in aquatic environments causes a serious problem for aquatic biota,  
42 especially fish. In water, the ammonia can be present in the ionized form ( $\text{NH}_4^+$ ) and un-  
43 ionized form ( $\text{NH}_3$ ), and both of these substances are present in equilibrium condition  
44 according to the following equation <sup>1</sup>:



46 The total concentration of the ionized ammonia ( $\text{NH}_4^+$ ) and un-ionized ammonia ( $\text{NH}_3$ ) in  
47 water is defined as the total ammonia nitrogen (TAN), and at a certain concentration the un-  
48 ionized ammonia ( $\text{NH}_3$ ) is lethal for fish. The equilibrium concentration of ammonia in the  
49 water is affected by both the pH and temperature. At high pH, the equilibrium condition  
50 (equation 1) will shift towards the formation of ammonia, while at low pH the formation of  
51 ammonium ion ( $\text{NH}_4^+$ ) is dominant. For aquatic biota such as fish, the ammonium ion is  
52 relatively non-toxic compared to the ammonia. Ammonia also predominates when  
53 temperature is high while the ammonium ion predominates at low temperature.

54

55 In the aquaculture industry the quality of water is the most important parameter for the  
56 continuation of the industry. One of the important parameters for the quality of water is TAN  
57 as it is the major nitrogenous waste product of fish and also results from the decomposition of  
58 organic matter. As a natural byproduct of fish metabolism, ammonia can accumulate easily in  
59 an aquatic system and it has the tendency to block the transfer of oxygen from gills to the  
60 blood nerve system and cause gill damage. The excess ammonia in water also destroys the  
61 mucous producing membrane in fish and damages the internal intestinal surfaces. The  
62 presence of excessive amounts of ammonia in the aquatic environment causes eutrophication.

63

64 A number of processes are currently available for the removal of TAN from the aquatic  
65 environment, and the most widely used process is the adsorption process. This process offers  
66 several advantages over other available processes, such as high removal efficiency, the  
67 adsorbent can be re-used, it can be applied for a wide range of concentrations, and is a cost  
68 effective process. One of the available natural adsorbents which is widely employed for the  
69 removal of ammonia from aquatic environment is a zeolite. A zeolite is a microporous  
70 aluminosilicate mineral which possesses a structure like a three-dimensional honeycomb with  
71 an overall negatively charged framework. The presence of hydrated alkali and/or alkaline  
72 earth cations ( $\text{Na}^+$ ,  $\text{K}^+$ ,  $\text{Ca}^{2+}$ ,  $\text{Mg}^{2+}$ ) in the pores of the aluminosilicate framework stabilizes  
73 the structure, and in the aquatic condition, these cations are also exchangeable with other  
74 cations from the solution <sup>2,3</sup>.

75

76 The disadvantage of using a natural zeolite as an adsorbent for the removal of  $\text{NH}_4^+$  ion from  
77 aqueous solution is a low adsorption capacity; most have a value less than 10 mg/g <sup>4-10</sup>. The  
78 low adsorption capacity and removal efficiency are still the main problem for industrial  
79 application of natural zeolites in aquaculture, water and wastewater processes. In order to  
80 improve the adsorption capacity, a modification using a chemical treatment processes is  
81 necessary such as using an acid, alkali or salt <sup>11-14</sup>. Microwave irradiation <sup>15</sup> and heat  
82 treatment <sup>16</sup> methods have also been employed to increase the adsorption capacity of natural  
83 zeolites. Leyva-Ramos *et al.* <sup>14</sup> modified natural zeolite chabazite with sodium chloride to  
84 remove ammonium from aqueous solution and the result clearly indicates that chabazite  
85 enriched with  $\text{Na}^+$  is more preferentially exchanged by  $\text{NH}_4^+$  than the other alkali cations.  
86 The modification using acid solution is seldom used because acid treatment causes de-  
87 alumination, the removal of  $\text{Al}^{3+}$  ions from the zeolite structure degrades it and decreases the  
88 ion exchange capacity <sup>1</sup>.

89

90 In this study a modification of natural mordenite with sodium hydroxide combined with a  
91 thermal treatment is investigated. To the best of our knowledge, this is the first of the use of  
92 such a modified zeolite as the adsorbent for removal of the ammonium ion from aqueous  
93 solution in an aquaculture system (Koi pond). Since the final goal of this study was to treat  
94 the ammonia from the Koi pond, therefore all of the adsorption experiments were conducted  
95 at a pH similar to the water of Koi pond system (6.5). The adsorption isotherms of  
96 ammonium ion onto natural and modified mordenite were obtained at three different  
97 temperatures (303.15, 308.15, and 313.15 K). The temperature-dependent forms of the  
98 Langmuir, Freundlich, Sips, and Toth equations were used to correlate the experimental  
99 adsorption data. The adsorption kinetics of ammonium ions onto the natural and modified  
100 zeolite was also studied. Well known pseudo first- and second-order kinetic models were  
101 employed to represent the kinetic data. The removal of ammonium ion from the Koi pond  
102 system was conducted in dynamic mode. The breakthrough adsorption performances were  
103 correlated by a Thomas equation.

104

## 105 **MATERIAL AND METHOD**

### 106 *Materials*

107 The natural zeolite used in this study was obtained from Ponorogo, East Java, Indonesia. The  
108 zeolite was crushed in a mortar and sieved using a Retsch Haan vibrator screener to particle  
109 size of about 0.85 - 1.70 mm (- 12 + 20 US mesh). All of the chemicals used in this study  
110 were obtained as pure analysis reagents from Sigma Aldrich Singapore and used without any  
111 further treatment or purification.

112

### 113 *Modified zeolite preparation*

114 The modification of the natural zeolite was performed under alkaline condition using sodium  
115 hydroxide solution at concentrations of 1 M, 3 M, and 6 M at 75°C for 24 h. Subsequently the  
116 modified zeolite was washed using tap water to remove excess sodium hydroxide solution.  
117 Then, the solid sample was dried at 110°C for 24 h.

118

### 119 *Characterization of solid samples*

120 The characterization of the natural (NatZ) and modified zeolites (1M-Z, 3M-Z, and 6M-Z)  
121 used scanning electron microscopy (SEM), X-ray diffraction (XRD), and nitrogen sorption.  
122 The SEM analysis was conducted to study the surface topography and texture of the  
123 adsorbents. The SEM analysis was conducted on a JEOL JSM-6390 field emission SEM  
124 operated at an accelerating voltage of 15 kV. Prior to analysis the samples were coated with  
125 ultra-thin layer of conductive platinum on the specimens using an auto fine coater (JFC-1200,  
126 JEOL, Ltd., Japan) for 120 s in an argon atmosphere. The X-ray diffraction analysis was  
127 conducted on a Philips PANalytical X'Pert powder X-ray diffractometer with  
128 monochromated high intensity Cu K $\alpha_1$  radiation ( $\lambda = 0.15406$  nm). The diffractograms were  
129 obtained at 40 kV, 30 mA and with a step size of 0.05°/s. The elemental compositions of the  
130 adsorbents were analyzed using a Bruker S8 Tiger X-ray fluorescence spectrophotometer.

131

132 The pore structures of NatZ, 1M-Z, 3M-Z, and 6M-Z were characterized by nitrogen sorption  
133 method. The nitrogen sorption measurements were carried out at boiling point of liquid  
134 nitrogen (77 K) on automated Micromeritics ASAP2010 sorption equipment. Prior to the  
135 analysis, the solid samples were degassed at 473.15 K for 24 h. The specific surface area of  
136 the samples were calculated by the Brunauer–Emmett–Teller (BET) method at a range of  
137 relative pressure of 0.05 to 0.3, while the total pore volume was determined at a relative  
138 pressure of 0.995.

139

140 *Adsorption isotherm study*

141 The adsorption isotherm study was conducted in batch mode at three different temperatures  
142 (303, 308, and 313 K) and pH of 6.5. A known amount of adsorbent (0.1 to 1.0 g) was added  
143 in a series of Erlenmeyer flasks containing 100 mL ammonium chloride solution with a  
144 concentration of 10 mg/L. The flasks were moved to a Memmert type WB-14 thermostatic  
145 shaker water bath. The temperature of the thermostatic shaker water bath was adjusted to a  
146 desired temperature and then the system was shaken at 100 rpm for 24 h (equilibrium  
147 condition). The equilibrium condition was determined at temperature of 303 K, pH of 6.5,  
148 and initial solution concentration of 10 mg/L. After the equilibrium time was reached, the  
149 solid adsorbent was removed from the solution by centrifugation. The concentration of  
150 ammonium in the solution was measured quantitatively at maximum wavelength (699.5 nm)  
151 based on Nessler method<sup>17</sup> using Shimadzu UV/VIS-1700 Pharma Spectrophotometer. The  
152 amount of ammonium ion adsorbed by the adsorbent at equilibrium condition was calculated  
153 by the following equation:

$$154 \quad q_e = \frac{(C_o - C_e)}{m} V \quad (2)$$

155 Where  $q_e$  is the equilibrium condition (mg/g),  $C_o$  (mg/L) and  $C_e$  (mg/L) are the initial and  
156 equilibrium concentration of ammonium in the solution, respectively. The amount of  
157 adsorbent (g) and the volume of solution (L) are represented by symbols  $m$  and  $V$ . The  
158 adsorption isotherm experiments were conducted in triplicate.

159

160 *Adsorption kinetic study*

161 The adsorptions kinetic of ammonium from aqueous solutions onto natural and modified  
162 zeolites were also conducted isothermally at three different temperatures (303, 308, and 313  
163 K) and pH of 6.5. A similar procedure to the adsorption isotherm study was employed for the



164 kinetic study. In the kinetic study, the fixed amount of adsorbent (1 g) was added to each  
165 Erlenmeyer containing 100 mL ammonium solution (10 mg/L). At a certain interval of time  
166 (1 h) one of the available flasks was taken from the thermostatic water bath. The amount of  
167 the ammonium adsorbed by the adsorbent at time  $t$  was determined by the following equation

$$168 \quad q_t = \frac{(C_o - C_t)V}{m} \quad (3)$$

169 Where  $C_t$  is the concentration of ammonium in the solution at time interval of  $t$ . The  
170 adsorption kinetic experiments were conducted in triplicate.

171

### 172 *Continuous adsorption experiment*

173 Continuous adsorption of ammonium ion from aqueous solution and Koi pond onto modified  
174 zeolites were conducted as follow: The modified zeolites were packed in glass columns of 1  
175 cm diameter and 16.5 cm height. Synthetic ammonium chloride solution and fish pond  
176 wastewater were pumped into the column using a Masterflex 7550-62 peristaltic pump. This  
177 experiment was performed to obtain breakthrough curves of ammonium from aqueous  
178 solution and real aquaculture system (in this case Koi pond). The flowrate of the solution  
179 entering the column was 6.5 mL/min and the height of modified zeolite in the column was 5  
180 cm. The solution was collected at the outlet of the column after certain intervals of time and  
181 the concentration of ammonium was measured spectrophotometrically using the Nessler  
182 method<sup>17</sup>.

183

## 184 **RESULTS AND DISCUSSION**

### 185 *Characterization of natural and modified zeolite*

186 The SEM micrographs of the surface morphology of NatZ and 6M-Z are depicted in Figure 1.  
187 It can be seen that the modification using a strong sodium hydroxide solution (6 M) did not  
188 affect the surface topography of the zeolite. The breakdown of some of the particles from a

189 needle-like shape into smaller and less uniform particles is attributed to the mechanical force  
190 used during the grinding of the zeolite.

191

192 The XRD patterns of NatZ and 6M-Z are given in Figure 2. The identification of the mineral  
193 content by comparing to the standard of JCPDS 80-0642 indicates it consists mainly of  
194 mordenite. The modification of the natural zeolite using sodium hydroxide solution did not  
195 change or degrade the mordenite as seen in the XRD patterns in Figure 2. This evidence  
196 clearly indicates that the sodium hydroxide modification exerted little or no influence on the  
197 crystallinity of the mordenite. The chemical composition of the natural zeolite and its  
198 modified form obtained from XRF analysis are summarized in Table 1. The increase of Na<sub>2</sub>O  
199 composition in modified zeolite indicates that the incorporation of exchangeable sodium ions  
200 to the natural zeolite occurred during the modification process. Partial exchange of several  
201 cations such as Ca<sup>2+</sup>, K<sup>+</sup> and, to a lesser extent, Mg<sup>2+</sup> with Na<sup>+</sup> was observed. With increasing  
202 NaOH concentration, the amount of CaO decrease from 2.43 to 0.11%, while the composition  
203 of Na<sub>2</sub>O increase from 1.87 to 3.85%. The modification using 6M NaOH almost completely  
204 transformed the Ca-zeolite into a Na-zeolite with, as stated earlier, no obvious change in  
205 crystallinity.

206

207 As illustrated in Figure 3, the modification of the natural zeolite using sodium hydroxide  
208 solution improved the porosity. The hysteresis loops in NatZ, 1M-Z, 3M-Z, and 6M-Z  
209 confirms the presence of mesopores in the pore structure. The BET surface area, micropore  
210 volume and total pore volume of the zeolites are summarized in Table 2. It can be seen that  
211 the micropores did not have significant contribution to the total pore since the values were  
212 almost equal to zero. The modification of zeolite using sodium hydroxide at 75°C brought the  
213 formation of more mesopores due to the clearing of the pore channels and voids of the natural

214 zeolite. The increased NaOH concentration also increased the formation of pores, leading to  
215 the increase of BET surface area and total pore volume as indicated in Table 2 and Figure 3.

216

#### 217 *Effect of sodium hydroxide concentration to adsorption capacity*

218 Initial adsorption experiments showed that the adsorption of ammonium ions had reached  
219 equilibrium after 24 h. For subsequent adsorption experiments, 24 h was chosen as the  
220 equilibrium time. Figure 4 shows the removal efficiency of  $\text{NH}_4^+$  from the solution using  
221 natural and NaOH modified zeolites as the adsorbents. This figure clearly indicates that  
222 NaOH modification effectively improved the adsorption capability of the zeolite for removal  
223 of  $\text{NH}_4^+$  from aqueous solution. According to Table 1, the removal efficiency of  $\text{NH}_4^+$  is  
224 closely related to the content of Na and Ca; the zeolite with higher Na and less Ca content  
225 removed more  $\text{NH}_4^+$ . Since the 6M-Z has the highest removal efficiency; this modified  
226 zeolite was used for subsequent adsorption experiments.

227

#### 228 *Adsorption equilibria*

229 The equilibrium relation between the ammonium ion on the surface of the adsorbent and in  
230 the solution could be related through an adsorption isotherm. Different kind of adsorption  
231 models have been developed and are currently used for the interpretation of liquid phase  
232 adsorption experimental data. The adsorption of chemical compounds onto the surface of  
233 adsorbents is affected by temperature. For physical adsorption, the temperature gives a  
234 negative effect on the adsorption capacity of adsorbent, while for chemical adsorption the  
235 uptake increases with the increase of temperature. The influence of temperature on the  
236 amount uptake can be represented in the adsorption models through the inclusion of  
237 temperature dependent forms<sup>18-20</sup>. In this study, the Langmuir, Freundlich, Sips, and Toth

238 models with their temperature dependent forms were employed to correlate the adsorption  
239 equilibria of  $\text{NH}_4^+$  onto NatZ and 6M-Z.

240

241 The Langmuir equation is one of the most widely used adsorption equations to correlate  
242 liquid phase adsorption experimental data of various systems. Based on the theory of the  
243 adsorption on a flat surface, Langmuir developed an adsorption model which has the form as  
244 follows

$$245 \quad q_e = q_{\max} \left( \frac{K_L C_e}{1 + K_L C_e} \right) \quad (4)$$

246 Where  $q_{\max}$  is the maximum amount of adsorbate adsorbed by the adsorbent to achieve  
247 complete monolayer coverage of the adsorbent surface (mg/g), and  $K_L$  is the adsorption  
248 affinity (L/mg). The parameters  $q_{\max}$  and  $K_L$  are affected by temperature, and the  
249 mathematical forms of these parameters as function of temperature are as follow:

$$250 \quad q_{\max} = q_{\max}^o \exp(\delta(T_o - T)) \quad (5)$$

$$251 \quad K_L = K_L^o \cdot \exp\left(\frac{-E}{R \cdot T_o}\right) \quad (6)$$

252 Parameter  $q_{\max}^o$  represents the maximum adsorption capacity at a reference temperature  $T_o$ ,  
253 while temperature coefficient of expansion of the adsorbate is represented by parameter  $\delta$ .  
254 The affinity constant of Langmuir equation at reference temperature and heat of adsorption  
255 are given by symbols  $K_L^o$  and  $E$ , respectively.

256

257 The second equation used in this study to represent the adsorption equilibria data is the  
258 Freundlich isotherm. This equation is the earliest known empirical adsorption equation and  
259 widely used for heterogeneous systems and reversible adsorption processes. The Freundlich  
260 isotherm has the form

$$261 \quad q_e = K_F \cdot C_e^{1/n}$$

$$262 \quad (7)$$

263 Where  $K_F$  ((mg/g)(mg/L)<sup>-n</sup>) and  $n$  are parameters represent adsorption capacity and the  
264 adsorption intensity, respectively. Parameter  $n$  also indicates the heterogeneity of the system.

265 The temperature dependent forms of Freundlich equation are

$$266 \quad K_F = K_F^0 \cdot \exp\left(\frac{-\alpha \cdot R \cdot T}{A_0}\right) \quad (8)$$

$$267 \quad \frac{1}{n} = \frac{R \cdot T}{A_0} \quad (9)$$

268 Where  $K_F^0$  is the adsorption capacity at the reference temperature,  $\alpha/A_0$  is a constant.

269

270 The Sips equation was developed for predicting adsorption in heterogeneous systems, and  
271 this model is a combination of the Langmuir and Freundlich adsorption isotherm. The  
272 advantage of Sips equation is it has a finite limit. The Sips equation can be written as follows:

$$273 \quad q_e = q_{\max} \cdot \left[ \frac{(K_s \cdot C_e)^{1/n}}{1 + (K_s \cdot C_e)^{1/n}} \right] \quad (10)$$

274 Where  $K_s$  (L/mg)<sup>n</sup> is the adsorption affinity of Sips model, and  $n$  characterizes the  
275 heterogeneity of the system. When the value of  $n$  become unity, Eq (10) reduces to Eq (4).

276 The temperature dependent forms of Sips equation are represented by parameter  $q_{\max}$ ,  $K_s$  and  
277  $n$ . The temperature dependent of  $q_{\max}$  follows Eq (5) while for  $K_s$  and  $n$  are as follow

$$278 \quad K_s = K_s^0 \cdot \exp\left[\frac{E}{R \cdot T_0} \left(1 - \frac{T_0}{T}\right)\right] \quad (11)$$

$$279 \quad n = \frac{1}{\frac{1}{n_0} + \eta \cdot \left(1 - \frac{T_0}{T}\right)} \quad (12)$$

280 The parameter  $K_s^o$  is a measure of the affinity between the adsorbate and the adsorbent at the  
 281 reference temperature, while  $n_o$  characterizes the heterogeneity of the system at reference  
 282 temperature. The parameter  $\eta$  is a constant of Sips temperature dependent form.

283

284 The last model used in this study is the Toth equation. This equation was developed on the  
 285 basis of potential theory and provides a good description of many systems with sub-  
 286 monolayer coverage<sup>21</sup>. Similar to Langmuir equation, Toth equation has finite saturation limit  
 287 for high concentration and follows Henry's law at very low concentration<sup>19</sup>.

$$288 \quad q_e = \frac{q_{\max} \cdot C_e}{(K_{Th} + C_e^t)^{1/t}} \quad (13)$$

289 The adsorption affinity of the Toth equation is given by parameter  $K_{Th}$  (mg/L)<sup>t</sup>, and  $t$  is a  
 290 parameter represents the system heterogeneity. Both of these parameters are affected by  
 291 temperature and can be written as:

$$292 \quad K_{Th} = K_{Th}^o \cdot \exp \left[ \frac{E}{R \cdot T_0} \left( \frac{T_0}{T} - 1 \right) \right] \quad (14)$$

$$293 \quad t = t_0 + \eta \cdot \left( 1 - \frac{T_0}{T} \right) \quad (15)$$

294 Where  $K_{Th}^o$  and  $t_0$  are adsorption affinity constant and parameter characterizes system  
 295 heterogeneity at reference temperature, respectively.

296

297 Temperature has a pronounced effect on the removal capacity of the zeolite as shown in  
 298 Figure 5 for NatZ and 6M-Z. The uptake of  $\text{NH}_4^+$  ions by both of the adsorbents decreased as  
 299 the temperature increased. The main mechanism of the adsorption of  $\text{NH}_4^+$  ions by the zeolite  
 300 is ion exchange and the process can be written as



302 In most cases, ammonium exchange onto a zeolite is an exothermic process<sup>5,8,22</sup>, therefore  
303 the increase of temperature will shift the equilibrium condition towards endothermic, and less  
304  $\text{NH}_4^+$  ions adsorbed by the NatZ and 6M-Z.

305

306 Figures 6 and 7 depict the adsorption equilibria of ammonium ions onto NatZ and 6M-Z at  
307 three different temperatures. The experimental data were fitted by temperature dependent  
308 forms of Langmuir, Freundlich, Sips, and Toth equations. The parameters of each model  
309 were obtained by the non-linear least-squares method, and the fitting was conducted for all  
310 the experimental data at various temperatures simultaneously using  $T_o = 298$  K. The Toth  
311 equation with its temperature dependent forms failed to correlate the adsorption equilibria  
312 data of ammonium onto NatZ. The values of parameters of Langmuir, Freundlich, Sips, and  
313 Toth equations obtained from the fitting of the adsorption experimental data are summarized  
314 in Table 3. Since the Toth equation failed to represent the adsorption equilibria data of  
315 ammonium onto NatZ, it will be excluded for further discussions of the validity of the  
316 adsorption equations in representing the adsorption experimental data.

317

318 Visually (Figures 6 and 7), Langmuir, Freundlich, and Sips isotherm equations could  
319 represent the experimental data well with good value of  $R^2$  (Table 3). However, the decision  
320 of the suitability of the models in representing the experimental data should not be based on  
321 the visual appearance of the model or the value of  $R^2$  but should be based on the physical  
322 meaning of the parameters obtained through the fitting of the data. The parameter  $q_{max}^0$  in the  
323 Langmuir and Sips models and the parameter  $K_F^0$  in the Freundlich model represent the  
324 adsorption capacity of the adsorbent at 298 K. Since the values of adsorption capacity of  
325 NatZ and 6M-Z were in the range of the adsorption capacity of common zeolites<sup>15,23</sup>,

326 therefore, the value of parameter  $q_{\max}^0$  and  $K_F^0$  of those models were physically consistent  
327 and reasonable.

328

329 The affinity parameter in the Langmuir and Sips models is expressed as  $K_L^0$  and  $K_S^0$ ,  
330 respectively. This parameter measures how strong the adsorbate (ammonium ion) is attracted  
331 to the adsorbent (zeolite) surface. A higher value of the affinity parameter means more  
332 adsorbate molecules cover the adsorbent surface. The experimental results revealed that 6M-  
333 Z zeolite has better adsorption capability than NatZ as seen in Figures 6 and 7. It indicates  
334 that 6M-Z zeolite had higher affinity value than NatZ. Based on the affinity parameter values  
335 listed in Table 3, all of three model used still capable to correlate the adsorption experimental  
336 data.

337

338 The parameter  $\delta$  in the Langmuir and Sips equations is the temperature coefficient of  
339 adsorbate expansion. The value this parameter is specific for different component and  
340 independent with type of adsorbent<sup>24</sup>. From Table 5, the fitted values of parameter  $\delta$  of  
341 ammonium ion obtained from both adsorbents and equations were essentially constant and  
342 consistent with the value of most liquids and independent on the type of adsorbent. Therefore,  
343 the Langmuir and Sips models still had plausible reason for further discussion.

344

345 In the Freundlich and Sips models, the heterogeneity of a given system is represented by  $A_0$   
346 (Freundlich) and  $n_0$  (Sips). The attachment and exchange of the sodium ion into the zeolite  
347 framework would increase the system heterogeneity, and therefore increase the  $A_0$  and  $n_0$   
348 value. The inconsistency of the heterogeneity parameter values with the physical meaning of  
349 this parameter is observed as indicated in Table 3. Since both of the Freundlich and Sips



350 models failed to predict a correct value, both of these are excluded in the subsequent  
351 discussion.

352

353 Figures 6 and 7 show that the temperature had a negative effect on the amount of ammonium  
354 ion uptake by both of NatZ and 6M-Z. This phenomenon indicates that physical adsorption is  
355 more dominant than chemisorption. Comparing the heat of adsorption value ( $E$ ) with  
356 adsorption bonding type is necessary to verify the adequacy of Langmuir isotherm model. An  
357 adsorption process can be classified into physical adsorption if the adsorption energy is less  
358 than 40 kJ/mol and chemisorption when the adsorption energy is between 40-80 kJ/mol. In  
359 physical adsorption, increasing temperature would weaken the interaction between adsorbate  
360 and adsorbent therefore less amount of ammonium ion adsorbed onto zeolite. The fitted  
361 adsorption heat value in Langmuir model was found to be consistent with the theory.  
362 Accordingly, Langmuir model can represent the adsorption data better than any other models.

363

#### 364 *Adsorption kinetic study*

365 The adsorption kinetic information is important for the design of an adsorption system. The  
366 rate of ammonium ion adsorbed into NatZ and 6M-Z are represented by pseudo-first order<sup>25</sup>  
367 and pseudo-second order<sup>26-28</sup> models. The pseudo-first order has the form

$$368 \quad q(t) = q_e \cdot (1 - \exp(-k_1 \cdot t)) \quad (17)$$

369 While the pseudo-second order has the following form

$$370 \quad q(t) = q_e \cdot \left( \frac{q_e \cdot k_2 \cdot t}{1 + q_e \cdot k_2 \cdot t} \right) \quad (18)$$

371 While  $k_1$  (1/hour) and  $k_2$  (g/mg.hour) are time scaling factor for pseudo-first and pseudo  
372 second order, respectively. Time scaling factor describes how fast the system reaches the  
373 equilibrium.

374

375 The adsorption kinetic data of  $\text{NH}_4^+$  onto NatZ and 6M-Z are given in Figures 8 and 9. Figure  
376 8 depicts the experimental data and plots of pseudo-first order while the plots of pseudo-  
377 second order are given in Figure 9. The fitted parameters of pseudo-first and pseudo-second  
378 order are given in Table 4. From Figures 8 and 9 and Table 4, it can be seen that pseudo-first  
379 order gave better performance in representing the experiment kinetic data than pseudo-second  
380 order. The deviation of  $q_e$  obtained from the fitting and experimental data in the pseudo first  
381 order is smaller than the pseudo-second order. Based on this evidence, the controlling  
382 mechanism of the adsorption of  $\text{NH}_4^+$  from aqueous solution onto NatZ and 6M-Z was  
383 dominated by physical adsorption.

384

385 Depending on the adsorption mechanism, the time scaling parameter  $k_1$  in pseudo-first order  
386 and  $k_2$  in pseudo-second order is also as a function of temperature. At a temperature higher  
387 than  $30^\circ\text{C}$ , the physical adsorption gave a quite dominant effect in the adsorption of  $\text{NH}_4^+$   
388 onto NatZ and 6M-Z. In both kinetic models, the value of this time scaling parameter  
389 decreased with increasing of temperature, obviously, the higher temperature of the system,  
390 the longer time was needed for the system to reach equilibrium state.

391

#### 392 *Adsorption of ammonia from real aquaculture water*

393 In order to test the effectiveness of the modified zeolite for removal of  $\text{NH}_4^+$  from an aquatic  
394 environment, an adsorption study using a real aquaculture system, a Koi pond, was also  
395 conducted. The water capacity of the Koi pond was  $2\text{ m}^3$  and it was equipped with a filtering  
396 and biological system. The number of Koi in the pond was 45 Koi carp with an average weight  
397 of  $2.0\text{ kg/Koi}$ . With this high density of Koi, the average ammonia concentration in the Koi  
398 pond after 1 h feeding was  $4.2\text{ mg/L}$ . The pH in the Koi pond was 6.5. The zeolites used for

399 the adsorption of  $\text{NH}_4^+$  from the Koi pond were NatZ, 1M-Z, 3M-Z, and 6M-Z. The adsorption  
400 experiments were conducted at 30°C in a batch mode.

401

402 The water analysis of the Koi pond before and after zeolite adsorption is given in Table 5. It  
403 can be seen that the adsorption in this real system also involved the adsorption of other ions.  
404 The competition with other ions occurred through different reaction mechanisms so it  
405 decreases the removal efficiency of ammonium ions by the zeolites. For 6M-Z zeolite, the  
406 removal efficiency decrease from 81% to 66.9%. The comparison of the adsorption capacity  
407 of sodium hydroxide modified zeolite mordenite with other zeolite adsorbents toward the  
408 ammonium ion is given in Table 6. From this table it can be seen that the sodium hydroxide  
409 modified zeolite mordenite has better ammonium adsorption capacity than other zeolites.

410

#### 411 *Continuous adsorption experiment*

412 A breakthrough curve for ammonium provides the performance of adsorption in a packed bed  
413 column system. A number of models with different kinds of assumptions have been  
414 developed and tested for various adsorption systems. One of the models is the Thomas  
415 equation:

$$416 \quad \frac{C_t}{C_o} = \frac{1}{1 + \exp \left[ \left( \frac{K_{Th} \cdot q_{max} \cdot x}{Q} \right) - K_{Th} \cdot C_o \cdot t \right]} \quad (19)$$

417 Where  $K_{Th}$  is Thomas rate constant (mL/min.mg) and  $q_{max}$  is maximum adsorption capacity  
418 (mg/g).

419

420 The zeolite used for the breakthrough curve experiments was 6M-Z. The breakthrough  
421 curves of the adsorption of  $\text{NH}_4^+$  from aqueous solution and from Koi pond water are given  
422 in Figure 10. The symbols represent the adsorption data while the solid lines represent the

423 Thomas model. From this figure it can be seen that the Thomas model can represent the  
424 experimental data well for both system. The values of parameters  $K_{Th}$  and  $q_{max}$  for adsorption  
425 of  $NH_4^+$  from the aqueous solution are 0.0082 mL/min.mg and 45.47 mg/g, respectively,  
426 while for the real system (Koi pond water) the values are  $K_{Th}$  and  $q_{max}$  of 0.0080 mL/min.mg  
427 and 38.40 mg/g, respectively.

428

429 The Thomas parameter  $K_{Th}$  for both systems is essentially the same, this parameter represents  
430 the interaction between adsorbent and adsorbate in a dynamic system. Since the breakthrough  
431 experiments for both systems were conducted at the same operating conditions (temperature,  
432 initial concentration, column diameter, and amount of adsorbent) it is not surprising that the  
433 parameter of  $K_{Th}$  for both systems should be the same. As mentioned before, the parameter  
434  $q_{max}$  represent the adsorption capacity of the adsorbent, the fitted value of  $q_{max}$  for adsorption  
435 of  $NH_4^+$  from aqueous solution is higher than from the Koi pond water. As seen in Table 5,  
436 the Koi pond water contains other ions besides  $NH_4^+$ . During the adsorption of  $NH_4^+$  in the  
437 packed bed column the competition for active sites or for exchangeable cations (especially  
438  $Na^+$ ) occurred; therefore less  $NH_4^+$  could be adsorbed/exchanged on the surface of 6M-Z. The  
439 breakthrough condition was achieved after 800 min.

440

## 441 CONCLUSIONS

442 The modification of natural zeolite from Ponorogo, predominantly mordenite, using NaOH as  
443 a modifying agent has been successfully conducted. The natural zeolite and its modified  
444 forms were used for the removal of ammonium ions from aqueous solution and Koi pond  
445 water. The adsorption and kinetic experiments were conducted at three different temperatures  
446 at static mode conditions. Temperature-dependent forms of Langmuir, Freundlich, Sips, and  
447 Toth adsorption equations were used to analyse the experimental data and among these

448 models the Langmuir model could best represent the data with reasonable values of the fitted  
449 parameters. For the kinetic study, well-known pseudo-first order and pseudo-second order  
450 equations were used to represent the kinetic data. Pseudo-first order gave better performance  
451 than pseudo-second order model. The Thomas model also successfully represents the  
452 dynamic adsorption data.

453

#### 454 **Acknowledgement**

455 The authors would like to acknowledge financial support for this work provided by  
456 Directorate of Higher Education, Indonesia Ministry of Research, Technology, and Higher  
457 Education through Competency Research Grant with project number  
458 003/SP2H/P/K7/KM/2015.

459

460

461

462

463

464

## 465 REFERENCES

- 466 1. Canadian Environmental Protection Act, *Ammonia in the Aquatic Environment Book*,  
467 1999.
- 468 2. A. Arslan and S. Veli, *J. Taiwan Inst. Chem. Eng.* 2012, **43**, 393-398.
- 469 3. M. Rozic, S. Cerjan-Stefanovic, S. Kurajica, V. Vancina, and E. Hodzic, *Water Res.*,  
470 2000, **34**, 3675-3681.
- 471 4. R. Malekian, J. Abedi-Koupai, S. S. Eslamian, S. F. Mousavi, K. C. Abbaspour, and  
472 M. Afyuni, *Appl. Clay Sci.*, 2011, **51**, 323-329.
- 473 5. K. Saltali, A. Sari, and M. Aydin, *J. Hazard. Mater.*, 2007, **141**, 258-263.
- 474 6. H. Huo, H. Lin, Y. Dong, H. Cheng, H. Wang, and L. Cao, *J. Hazard. Mater.*, 2012,  
475 **229-230**, 292-297.
- 476 7. L. Zhou, and C.E. Boyd, *Aquaculture*, 2014, **432**, 252-257.
- 477 8. A. Alshameri, A. Ibrahim, A.M. Assabri, X. Lei, H. Wang, and C. Yan, *Powder*  
478 *Technol.*, 2014, **258**, 20-31.
- 479 9. G. Moussavi, S. Talebi, M. Farrokhi, and R.M. Sabouti, *Chem. Eng. J.*, 2011, **171**,  
480 1159-1169.
- 481 10. M. Li, X. Zhu, F. Zhu, G. Ren, G. Cao, and L. Song, *Desalination*, 2011, **271**, 295-  
482 300.
- 483 11. Y.P. Zhao, T.Y. Gao, S.Y. Jiang, and D.W. Cao, *J. Environ. Sci.* 2004, **16**, 1001-  
484 1004.
- 485 12. Y. Watanabe, H. Yamada, J. Tanaka, and Y. Moriyoshi, *J. Chem. Technol.*  
486 *Biotechnol.* 2005, **80**, 376-380.
- 487 13. H.B. Wang, Y.M. Bao, J. Zhang, H.Y. Chen, L.Z. Ma, and M. Yang, *Energy*  
488 *Procedia*, 2011, **11**, 4236-4241.

- 489 14. R. Leyva-Ramos, J. E. Monsivais-Rocha, A. Aragon-Pina, M. S. Berber-Mendoza, R.  
490 M. Guerrero-Coronado, P. Alonso-Davila, and J. Mendoza-Barron, *J. Environ.*  
491 *Manage.*, 2010, **91**, 2662-2668.
- 492 15. Z. Liang, and J.R. Ni, *J. Hazard. Mater.*, 2009, **166**, 52–60.
- 493 16. L. Lei, X.J. Li, and X.W. Zhang, *Sep. Purif. Technol.*, 2008, **58**, 359–366.
- 494 17. APHA, *Water Environment Federation, Washington DC, USA*, 1998.
- 495 18. I. K. Chandra, Y.-H. Ju, A. Ayucitra, and S. Ismadji, *Int. J. Env. Sci. Technol.*, 2013,  
496 **10**, 359-370.
- 497 19. Yesi, F. P. Sisnandy, Y.-H. Ju, F. E. Soetaredjo, and S. Ismadji, *Ads. Sci. Technol.*,  
498 2010, **28**, 846-868.
- 499 20. A. C. Suwandi, N. Indraswati, and S. Ismadji, *Desal. Wat. Treatment*, 2012, **41**, 342-  
500 355.
- 501 21. Do, D.D. (1998) *Adsorption Analysis: Equilibria and Kinetics*, Imperial College Press,  
502 London, U.K.
- 503 22. M. Zhang, H. Zhang, D. Xu, L. Han, D. Niu, B. Tian, J. Zhang, L. Zhang, and W. Wu,  
504 *Desalination*, 2011, **271**, 111-121.
- 505 23. V.K. Jha, and S. Hayashi, *J. Hazard. Mater.*, 2009, **169**, 29-35.
- 506 24. S. Ismadji and S. K. Bhatia, *Langmuir*, 2001, **17**, 1488-1498.
- 507 25. S. Lagergren, *Handlingar*, 1898, **24**, 1-39.
- 508 26. Y.C. Sharma, G.S. Gupta, G. Prasad, and D.C. Rupainwar, *Water Air Soil Poll.*, 1990,  
509 **49**, 69-79.
- 510 27. M. Essandoh, B. Kunwar, C.U. Pittman Jr, D. Mohan, and T. Misna, *Chem. Eng. J.*,  
511 2015, **265**, 219-227.
- 512 28. C. Gan, Y. Liu, X. Tan, S. Wang, G. Zeng, B. Zheng, T. Li, Z. Jiang, and W. Liu,  
513 *RSC Adv.*, 2015, **5**, 35107-35115.

514 29. Y. Zhao, B. Zhang, X. Zhang, J. Wang, J. Liu, and R. Chen, *J. Hazard. Mater.*, 2010,  
515 **178**, 658-664.

516 30. H. Zheng, L. Han, H. Ma, Y. Zheng, H. Zhang, D. Liu, and S. Liang, *J. Hazard.*  
517 *Mater.*, 2008, **158**, 577-584.

518

519

520

521

522

523

524

525

526

527

528

529

530

531

532

533

534

535

536

537

538

539

540



541

542 **Table 1.** Chemical composition of natural and NaOH modified zeolites as determined by

543

XRF.

Element	% weight			
	NatZ	1M-Z	3M-Z	6M-Z
SiO <sub>2</sub>	60.85	60.14	62.05	58.47
Al <sub>2</sub> O <sub>3</sub>	11.78	12.03	12.6	13.41
CaO	2.43	1.92	0.93	0.11
Fe <sub>2</sub> O <sub>3</sub>	2.07	2.02	2.01	1.78
Na <sub>2</sub> O	1.87	2.34	3.05	3.85
K <sub>2</sub> O	1.05	0.95	0.92	0.51
MgO	0.52	0.51	0.51	0.42
Other	19.43	20.09	17.93	21.45

544

545

546

547

**Table 2.** The pore characteristics of natural and modified zeolites

Sample	S <sub>BET</sub> , m <sup>2</sup> /g	V <sub>micro</sub> , cm <sup>3</sup> /g	V <sub>Total</sub> , cm <sup>3</sup> /g
NatZ	30.2	0.002	0.116
1M-Z	38.9	0.002	0.138
3M-Z	49.5	0.002	0.153
6M-Z	58.6	0.002	0.182

548

549

550

551

552

553

554

555

556

557

558

559

560

561 **Table 3.** The parameters of Langmuir, Freundlich, Sips and Toth equations as fitted to the

562 adsorption of ammonium onto NatZ and 6M-Z

Isotherm Model	Parameters	NatZ	6M-Z
Langmuir	$q^0_{max}$ (mg/g)	7.9462	53.9169
	$\delta$ (K <sup>-1</sup> )	0.00203	0.00218
	$K_L^0$ (L/mg)	0.1111	0.4044
	$E$ (kJ/mol)	1.575	18.234
	$R^2$	0.9851	0.9882
Freundlich	$K_F^0$ (mg/g)(mg/L) <sup>-n</sup>	1.2505	1.676
	$\alpha/A_0$	0.029	-0.0412
	$A_0$	37.82	36.63
	$R^2$	0.9835	0.9925
Sips	$q^0_{max}$ (mg/g)	0.1166	0.5633
	$\delta$ (K <sup>-1</sup> )	0.00251	0.00243
	$K_S^0$ (L/mg)	4.0834	7.0279
	$E$ (kJ/mol)	0.8499	10.36
	$n_0$	1.4735	1.333
	$\eta$	-0.3281	-1.8641
	$R^2$	0.9835	0.9724
Toth	$q^0_{max}$ (mg/g)	-	528.567
	$K_{Th}^0$ (L/mg)		5.3859
	$E$ (kJ/mol)		31.327
	$t_0$		0.4155
	$\eta$		-2.6879
	$R^2$		0.929

563

564

565

566

567

568

569

570

571 **Table 4.** Fitted parameters for pseudo-first order and pseudo-second order for adsorption  
 572 kinetic of  $\text{NH}_4^+$  onto NatZ and 6M-Z

T (K)	Pseudo-first order			Pseudo-second order		
	$k_1$ (1/h)	$q_e$ (mg/g)	$R^2$	$k_2$ (g/mg.h)	$q_e$ (mg/g)	$R^2$
Using natural zeolite as adsorbent						
303	0.2399	2.9457	0.9785	0.0485	4.0609	0.9691
308	0.1929	2.9243	0.9602	0.0335	4.2665	0.9525
313	0.1837	2.7522	0.9656	0.0326	4.0744	0.9580
Using modified zeolite as adsorbent						
303	0.4102	20.7974	0.9796	0.0167	25.6145	0.9644
308	0.3764	20.3851	0.9733	0.0147	25.5650	0.9568
313	0.3480	20.1977	0.9698	0.0130	25.7437	0.9550

573

574

575

576

577

578

579

580

581

582

583

584

585

586 **Table 5.** Water analysis report of Koi pond before and after adsorption using zeolites

	Original	NatZ	1M-Z	3M-Z	6M-Z
pH	6.5 ± 0.0	6.5 ± 0.0	6.5 ± 0.0	6.5 ± 0.0	6.5 ± 0.0
Alkalinity total as CaCO <sub>3</sub> , mg/L	121 ± 4.1	121 ± 3.2	120 ± 5.5	121 ± 3.8	119 ± 2.1
CO <sub>3</sub> <sup>2-</sup> as CaCO <sub>3</sub> , mg/L	1.21 ± 0.04	1.21 ± 0.06	1.18 ± 0.05	1.11 ± 0.05	1.05 ± 0.03
Fe <sup>2+</sup> , mg/L	0.12 ± 0.01	0.11 ± 0.01	0.11 ± 0.02	0.08 ± 0.01	0.06 ± 0.0
Mn <sup>2+</sup> , mg/L	0.01 ± 0.0	0.01 ± 0.0	-	-	-
Cl <sup>-</sup> , mg/L	4.50 ± 0.08	4.42 ± 0.05	4.34 ± 0.07	4.24 ± 0.09	4.14 ± 0.21
SO <sub>4</sub> <sup>2-</sup> , mg/L	3.74 ± 0.14	3.69 ± 0.10	3.61 ± 0.09	3.43 ± 0.11	3.11 ± 0.23
NO <sub>3</sub> <sup>-</sup> , mg/L	0.09 ± 0.0	0.08 ± 0.0	0.07 ± 0.01	0.02 ± 0.0	-
Total ammonia, mg/L	4.20 ± 0.17	3.91 ± 0.13	3.25 ± 0.20	2.61 ± 0.05	1.39 ± 0.06
NO <sub>2</sub> <sup>-</sup> , mg/L	0.01 ± 0.0	-	-	-	-
PO <sub>4</sub> <sup>3-</sup> , mg/L	0.15 ± 0.01	0.14 ± 0.02	0.12 ± 0.01	0.11 ± 0.01	0.08 ± 0.01

587

588

589 **Table 6.** Adsorption capacity of sodium hydroxide modified zeolite mordenite and several

590

zeolites samples toward ammonium ion

Sample	Adsorption capacity, mg/g	References
zeolite mordenite	7.94	This study
sodium hydroxide modified zeolite mordenite	53.91	This study
New Zealand mordenite	8.70	7
Natural calcium rich zeolite	9.72	15
Sodium salt modified zeolite	15.44	
NaA zeolite from halloysite	44.30	29
Zeolite 13X	8.61	30

591

592

593

594

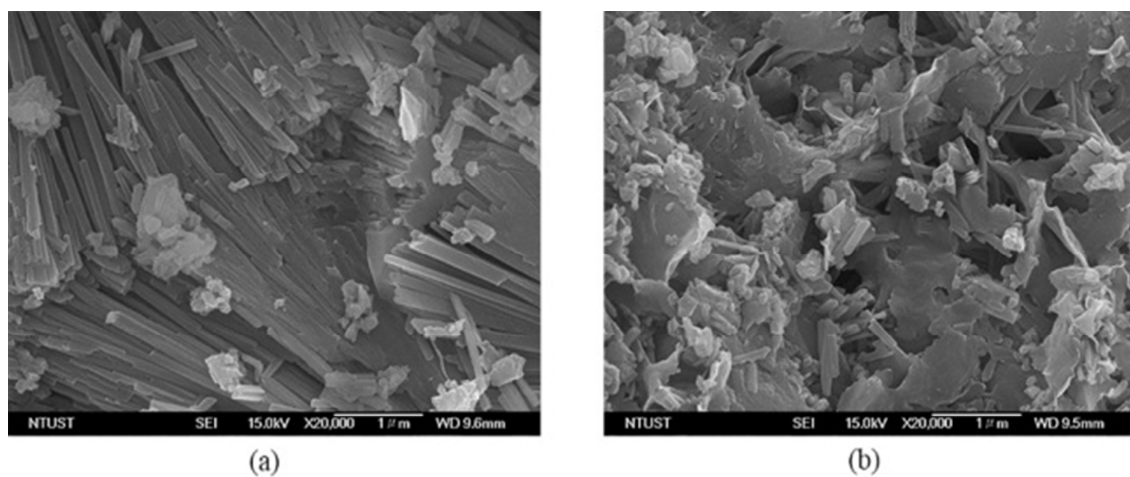
595

596

597

598

599



600

601 **Figure 1.** Surface topography of (a) natural zeolite (NatZ), and (b) modified zeolite (6M-Z)

602

603

604

605

606

607

608

609

610

611

612

613

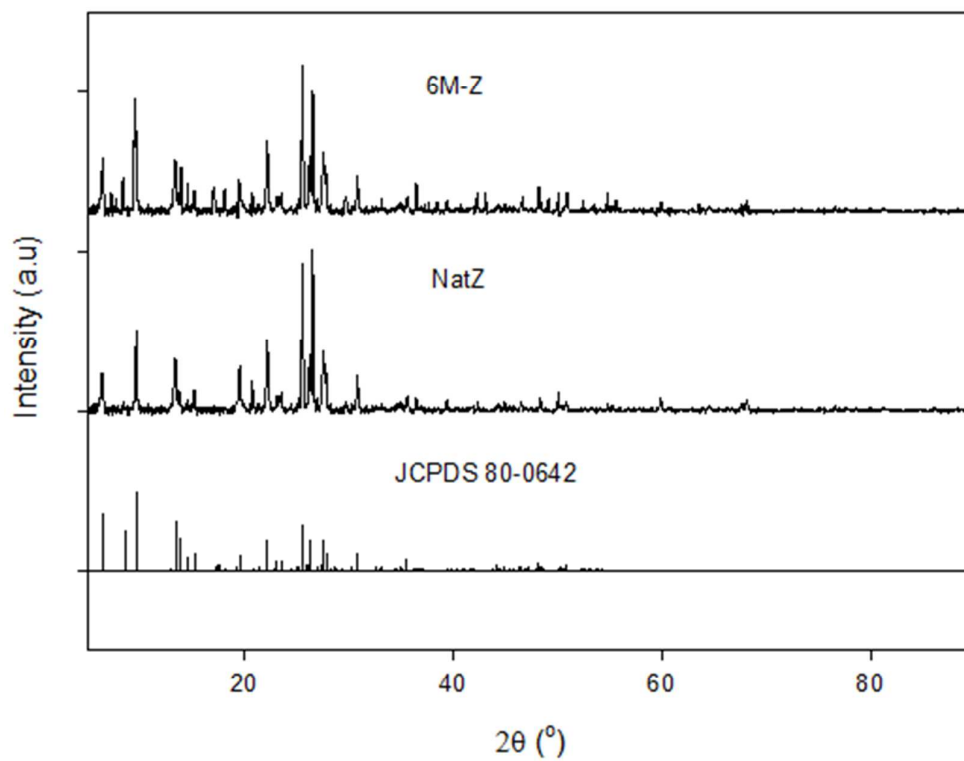
614

615

616

617

618



619

620 **Figure 2.** XRD diffractograms of natural zeolite (NatZ) and its modified form (6M-Z) with  
621 the pattern reported for mordenite in the ICSD JCPDS database.

622

623

624

625

626

627

628

629

630

631

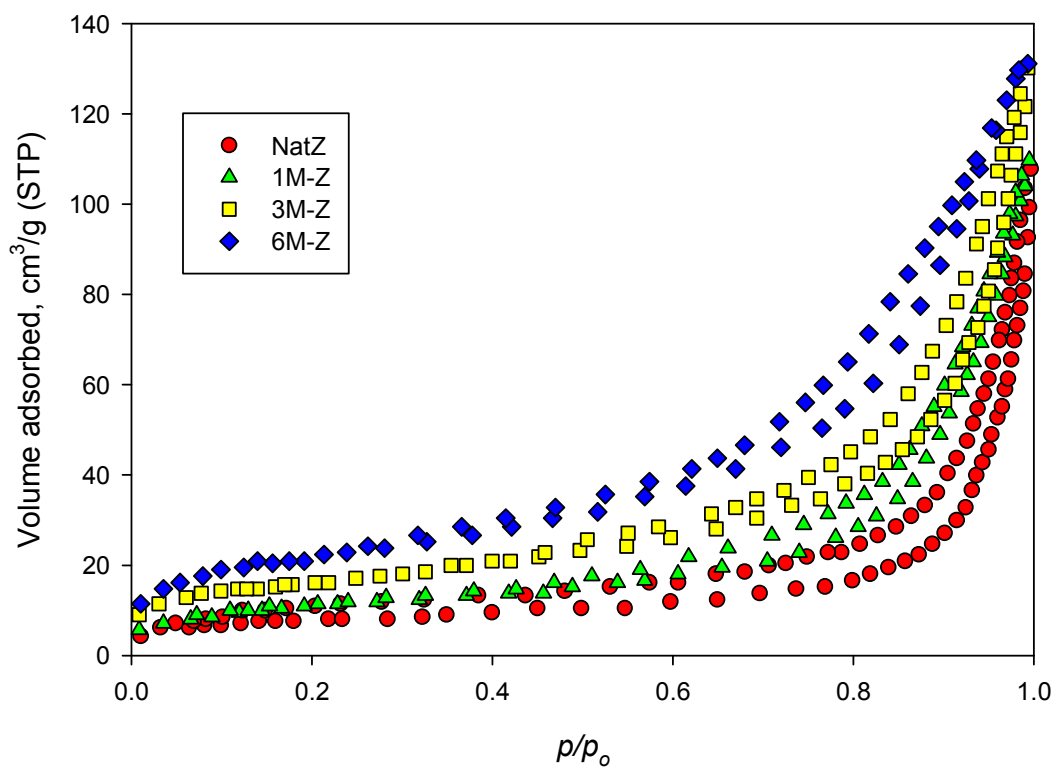
632

633

634

635

636



637

638 **Figure 3.** Nitrogen sorption isotherms of natural and modified zeolites

639

640

641

642

643

644

645

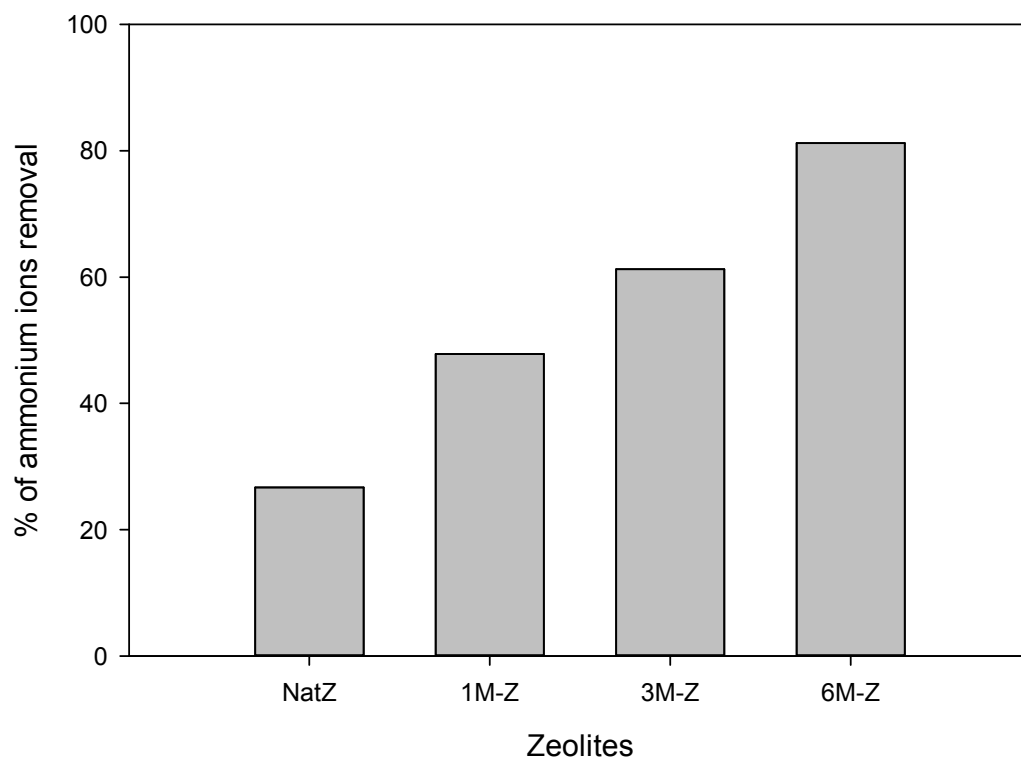
646

647

648

649

650



651

652

**Figure 4.** Removal efficiency of natural and modified zeolites

653

654

655

656

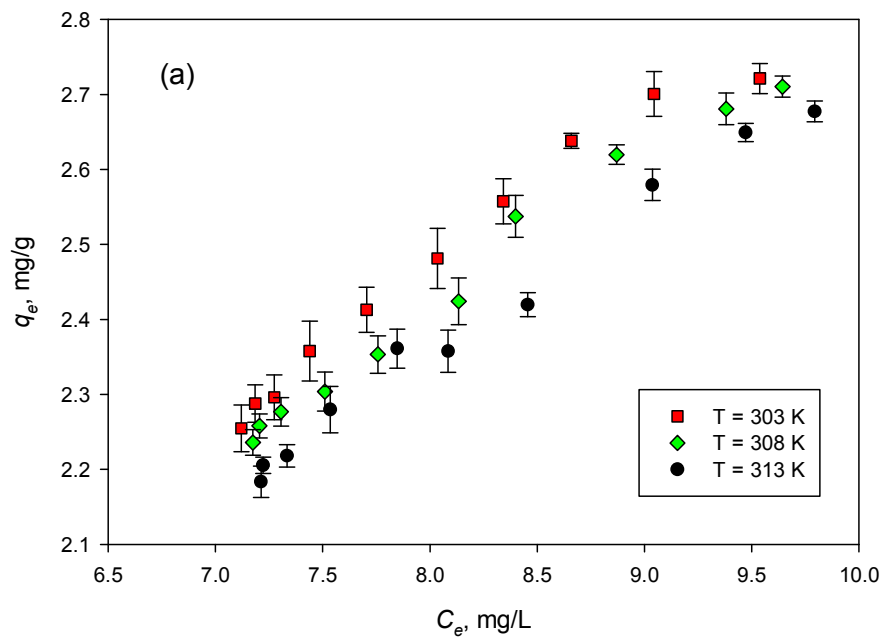
657

658

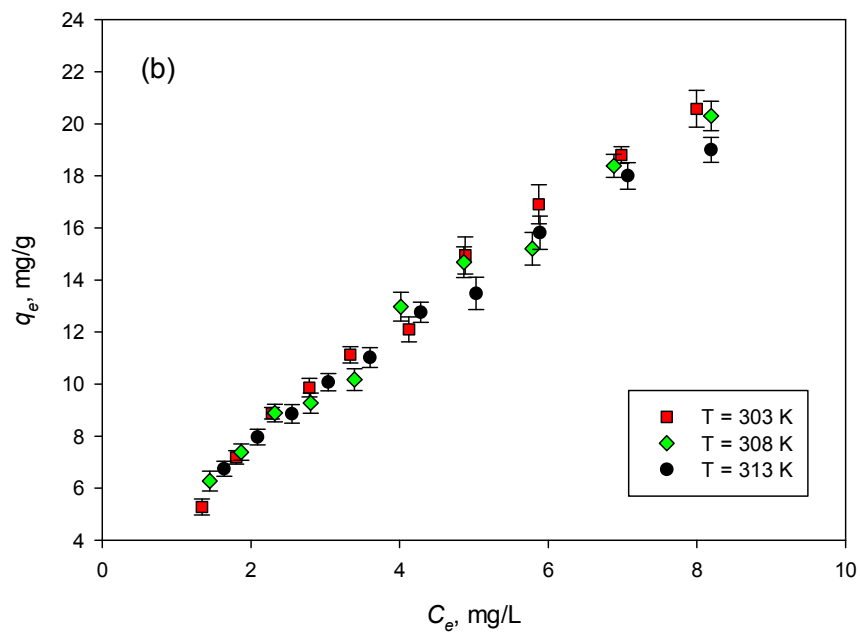


659

660



661



662

663

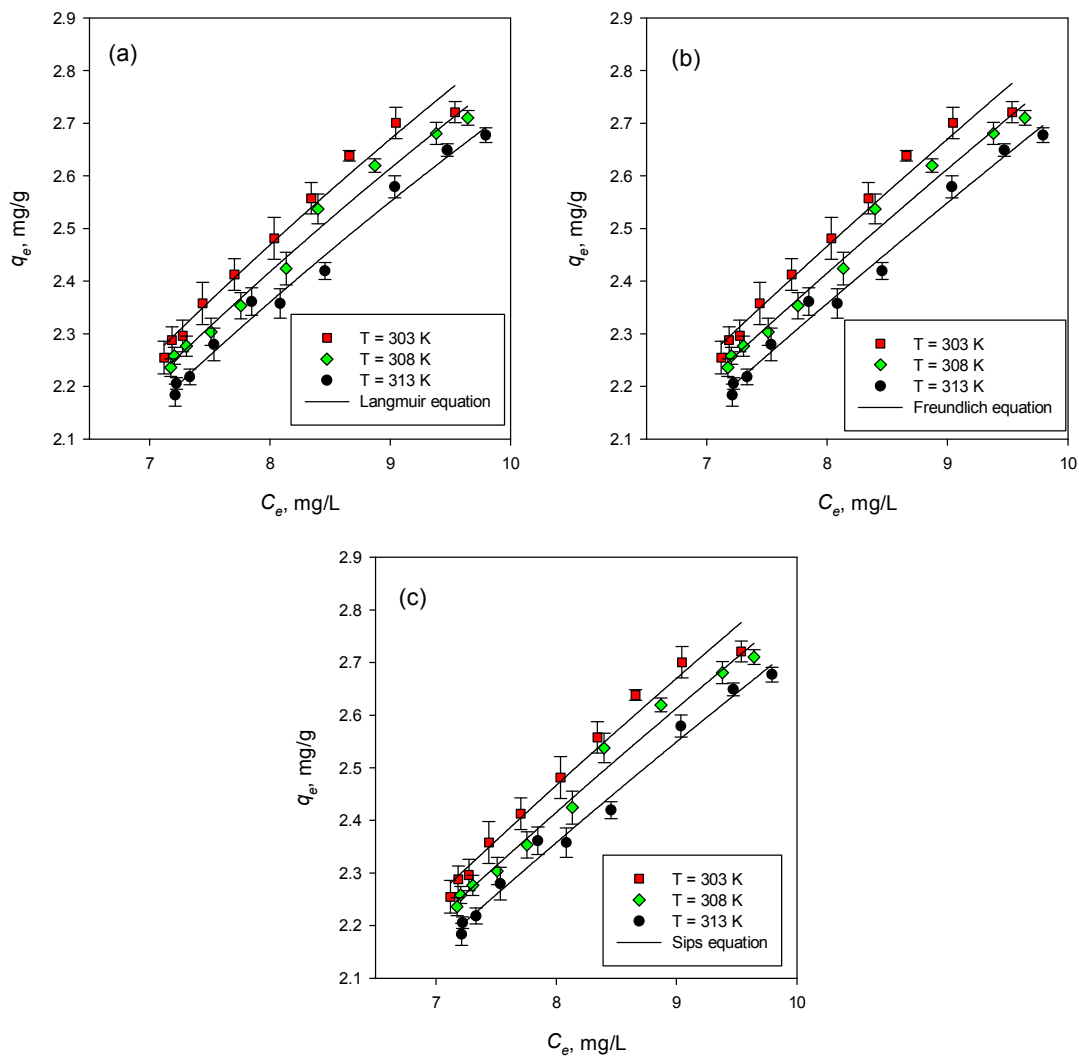
**Figure 5.** Effect of temperature on ammonium removal using: a) NatZ, b) 6M-Z

664

665

666

667



668

669 **Figure 6.** Adsorption experimental data of ammonium ion into NatZ and the model fitted by:

670

670 (a) Langmuir, (b) Freundlich, and (c) Sips.

671

672

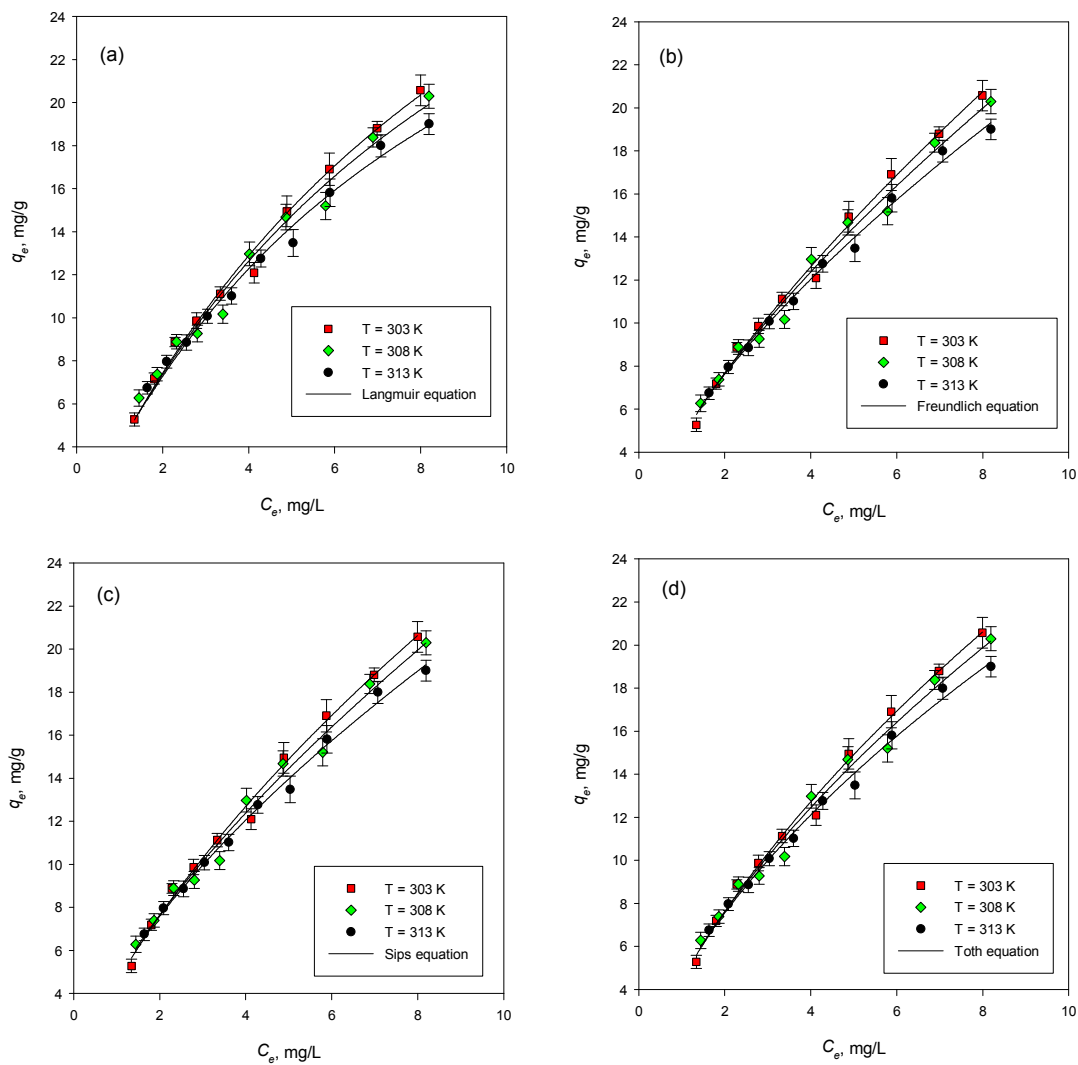
673

674

675

676

677



678

679 **Figure 7.** Adsorption experimental data of ammonium ion into 6M-Z and the model fitted by:

680

(a) Langmuir, (b) Freundlich, (c) Sips, and (d) Toth.

681

682

683

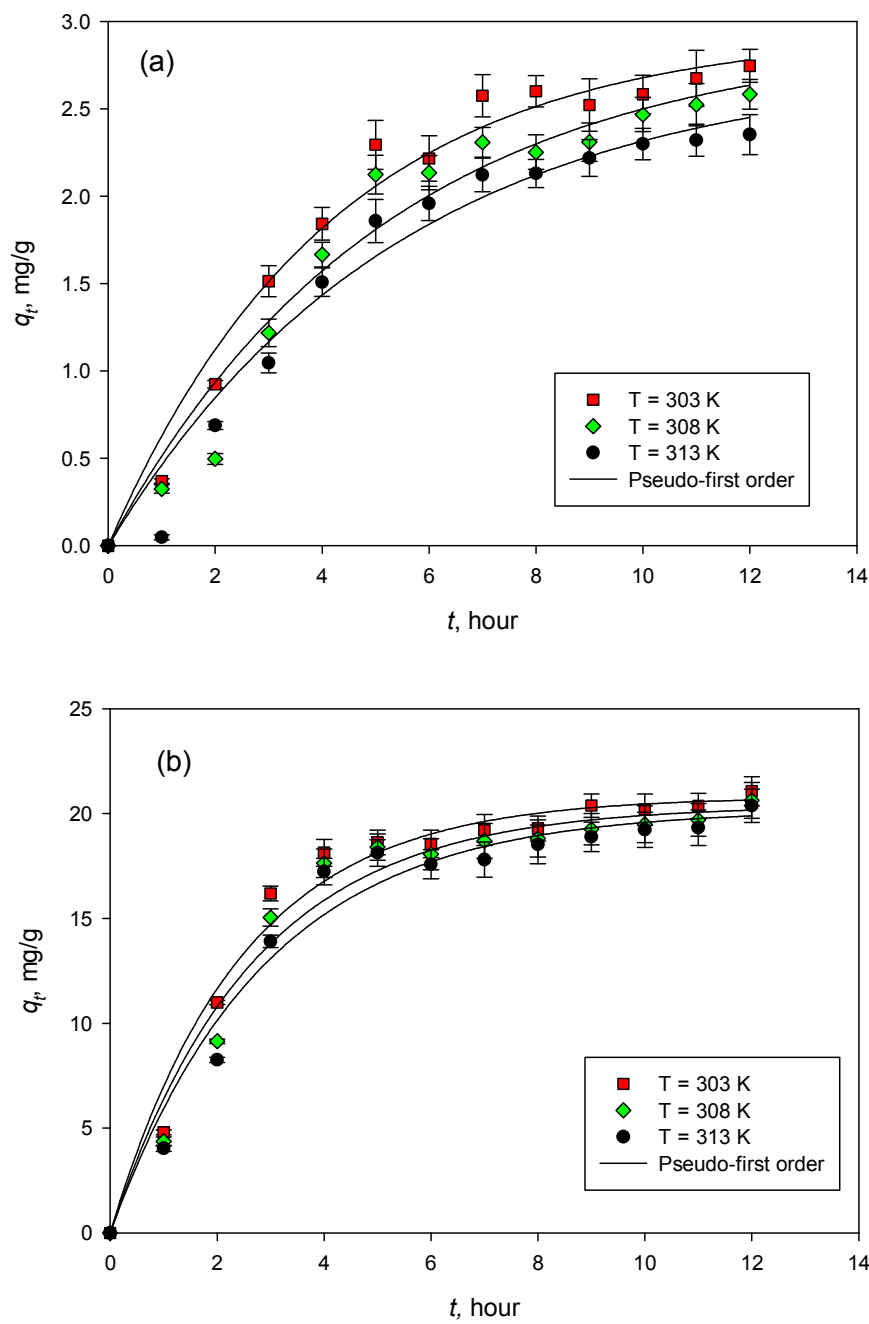
684

685

686

687

688



689

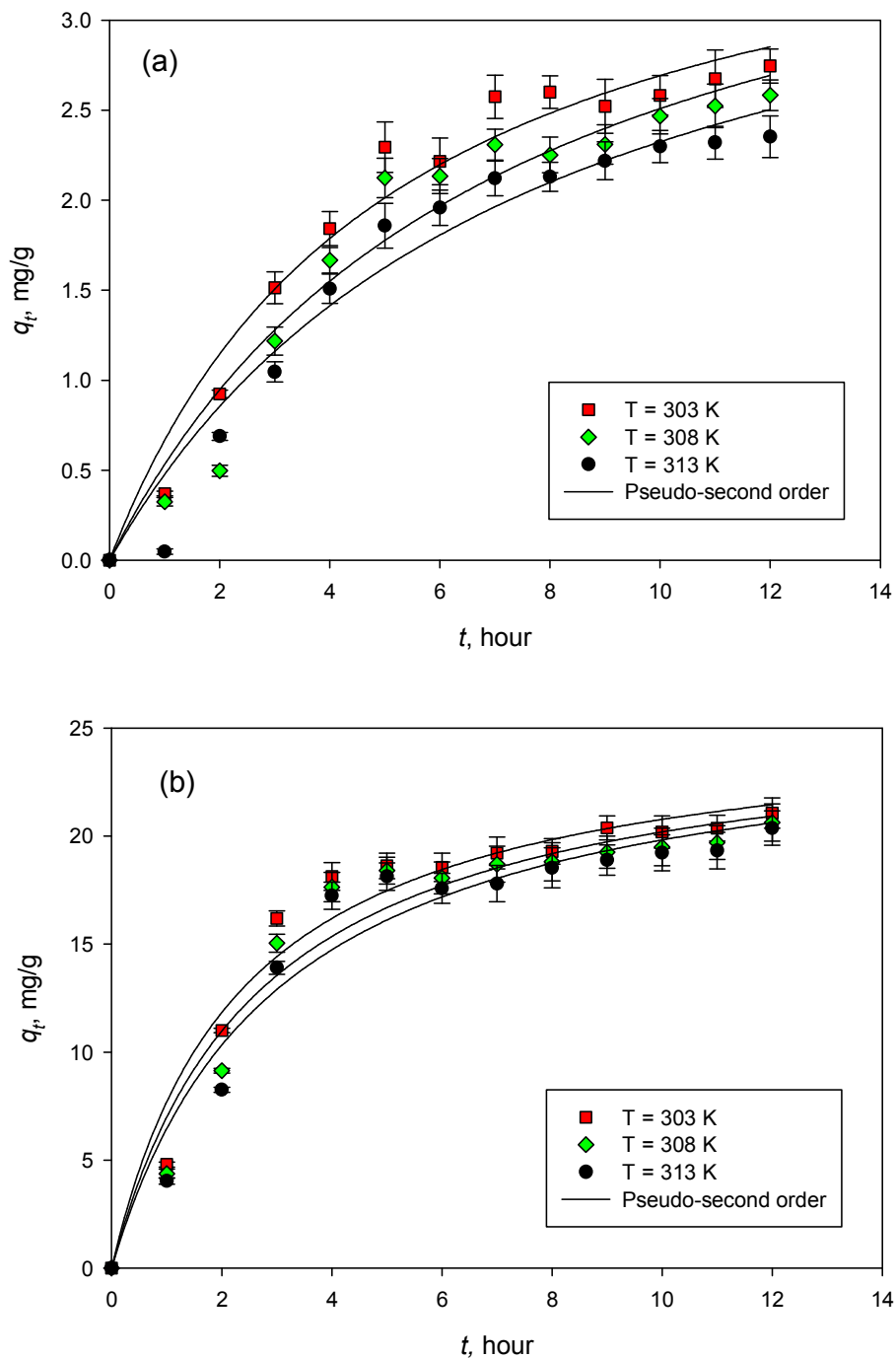
690 **Figure 8.** Pseudo first order reaction kinetics for the adsorption of  $\text{NH}_4^+$  ion on (a). NatZ and

691

(b). 6M-Z

692

693



694

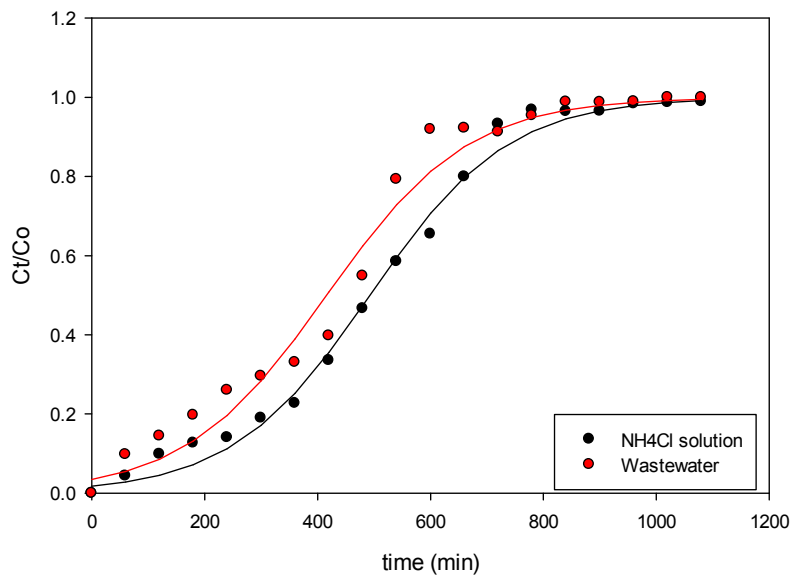
695 **Figure 9.** Pseudo second order reaction kinetics for the adsorption of  $\text{NH}_4^+$  ion on (a) NatZ

696

and (b) 6M-Z

697

698



699

700 **Figure 10.** Breakthrough curve for  $\text{NH}_4^+$  adsorption from aqueous solution and Koi pond  
701 water

702